Assiut University Journal of Chemistry (AUJC) 45(2016) 1-16

Journal homepage: www.aujc.org

(ISSN 1678-4919) (Print) (ISSN 2357-0415) (Online)

Vol(45)	No(1)	2016

Full Paper

Synthesis, characterization and DNA interaction of Ni(II) lysine Schiff-base complexes

S. A .Sallam, A.M. Abbas*
Chemistry Department, Faculty of Science, Suez Canal University, Ring Road 41511, Ismailia, Egypt.
E-mail *:* shehabsallam@yahoo.com

Article history: Received: 22/10/2015; Revised :7/12/2015; Accepted : 15/1/2016 ; Available Online : 23/5/2016 ;

Abstract
Ni(II) complexes with Schiff-bases obtained by the condensation of lysine with salicylaldehyde; 2,3-; 2,4- and 2,5-dihydroxybenzaldehyde and o-hydroxynaphthaldehyde have been synthesized using template method in ethanol or ammonia media. They are characterized by elemental analysis, conductivity measurements, magnetic moment, UV, IR, and ^{1}H NMR spectra as well as thermal analysis (TG, DTG, DTA). The Schiff-bases are dibasic tridentate donors and the complexes have square planar and octahedral structures. The complexes thermally decompose in two or three steps where kinetic and thermodynamic parameters of the decomposition steps are computed. The interactions of the formed complexes with FM-DNA were monitored using UV and florescence spectroscopy.

Keywords: Lysine Shiff-bases, Ni(II) complexes, magnetic, spectral and thermal properties, DNA interaction.

1. Introduction

Several structure studies have been carried out on transition metal complexes of Schiff-bases derived from salicylaldehyde and hydroxynaphthaldehyde with amino acids in view of the fact that these complexes can be used as non-enzymatic models analogous to the key intermediates in many metabolic reactions of amino acids such as transamination, decarboxylation, α- and β-elimination, racimization and intermediate products in biologically important reactions [1-5]. A series of novel heteronuclear Ln(III)-Cu(II) complexes with the general formulae $[LnCu_2(H_2TALY)(NO_3)_5](NO_3)_2.nH_2O$ (Ln=La, Nd, Sm, Gd; *n* = 4; Ln = Yb, Y; *n* = 3) and H_2TALY = tetraglycol aldehyde bis-lysine Schiff-base were synthesized and characterized [6]. Hetero bis-Shiff- base was obtained from lysine with salicylaldehyde on one side and o-vaniline on the other and twelve lanthanide complexes were also reported and discussed [7]. The complexes with the formulae $[Ln(TBLY)(NO_3)_3].nH_2O$ (Ln=La, n=3; Nd, n=5, Gd, Dy, Yb, Y; n=7) and TBLY=tetraglycol aldehyde-2,4-dihydroxybenzaldehyde bis-lysine Schiff-base were synthesized and characterized [8].

Schiff-base derived from phthaldehyde and lysine (L) and its complexes $LnL_2(NO_3).nH_2O$ (Ln=La, Pr, Nd, Sm, Y; *n*=4 and La=Gd, Tb, Dy, Er, Yb; *n*=3) were synthesized and characterized [9]. The unsymmetrical Schiff-base (H_2LLn) was synthesized using lysine, salicylaldehyde and 2-hydroxy-1-naphthaldehyde and three metal complexes$[Ln(H_2L)(NO_3)_2].NO_3.2H_2O$ (Ln=La, Sm, Ho) have been prepared and characterized [10]. Two complexes, $[Ln(HL)(H_2O)_2NO_3].NO_3.H_2O$ (Ln=La and Gd), where HL is a Schiff-base derived from o-vanillin and lysine, have been synthesizes and characterized and their interaction with CT-DNA was also investigated [11]. Iron(III) complex $[Fe(L)_2]Cl$ where L is monoanionic N-salicylidene-lysine (sal-lysH) were prepared and their DNA binding and photo-induced DNA cleavage activity studied [12]. In order to contribute to these studies, we have prepared –in solution– Schiff-bases of lysine (lys) with salicylaldehyde (sal); 2,3-diOH- ; 2,4-diOH- ; 2,5-diOH-benzaldehyde and o-OH-naphthaldehyde (o-OH-naph.). Ni(II) complexes of the Schiff-bases were synthesized by template reaction using alcohol or ammonia as solvents. They were characterized using elemental analysis, magnetic properties, spectral (IR, UV-Vis. and ^1H NMR) and thermal (TG, DTG and DTA) methods. The interaction between the Ni(II) complexes of the Schiff-bases and fish melt DNA (FM-DNA) under physiological conditions was investigated by UV and fluorescence spectroscopy.

2.Experimental

Lysine; salicylaldehyde; 2,3-diOH-; 2,4-diOH-; 2,5-diOH-benzaldehyde and o-hydroxynaphthaldehyde were purchased from Fluka, Aldrich and Merck. All solvents were of analytical grade reagents.

2.1.Preparation of the Schiff-bases

Lysine (1 mmol, 0.146 g) and 2 mmol of the corresponding aldehyde were dissolved in 10 ml of EtOH. The mixture solution was refluxed under stirring and pubbling of purified N_2 gas for two hours. The solution turns to yellow color indicating the formation of the Schiff-bases. We succeed to precipitate salicylaldenelysine Schiff-base but trials to precipitate the other Schiff-bases by evaporation of the solvent or using solvent mixture were unsuccessful.

2.2.Template Synthesis of the Ni(II) complexes

To the obtained Schiff-bases solutions (1 mmol) in EtOH medium, a solution of $NiCl_2.6H_2O$ (2 mmol, 0.5 g) in 10 ml EtOH was added with stirring and refluxed for 1 hour. After cooling, the solid complexes were precipitated which were washed with EtOH and $(EtO)_2$ and dried under vacuum. If we add ammonia solution (5 ml, 28%) before reflux of the mixture, we obtain another series of Ni(II) complexes in which NH_3 is the co-ligand instead of water.

2.3.Physical Measurements

C, H, and N were estimated using a Heraus CHN-rapid analyzer. The IR spectra were recorded (KBr disc) in the 400-4000cm^{-1} range on Bruker Vector-22 spectrometer. The electronic absorption spectra were obtained by nujol mull and 10^{-3}M DMF solution in 1cm quartz cell using UV-1601PC Shimadzu spectrophotometer. Magnetic susceptibility measurements were carried out using the modified Gouy method [13] on MSB-MK1 balance at room temperature using mercury(II)tetrathio-cyanatecobaltate(II) as standard. The effective magnetic moment, μ_{eff} , per metal atom was calculated from the expression $\boldsymbol{\mu}_{eff} = 2.83\sqrt{\chi.T}$ B.M., where χ is the molar susceptibility corrected using Pascal's constant for the diamagnetism of all atoms in the complexes. TGA, DTG and DTA were recorded on Shimadzu 60 thermal analyzer under a dynamic flow of nitrogen (30 ml/min.) and heating rate 10˚C/min. from ambient temperature to 750˚C. Electrical conductivity measurements were carried out at room temperature on freshly prepared 10^{-3}M DMSO solutions using WTW conductivity meter fitted with L100 conductivity cell. Metal content was obtained by EDTA titration using murexide indicator at pH 10 using ammonia buffer.

2.4.DNA Interaction

Experiments were carried out in Tris–HCl buffer at pH 7.0. A solution of fish melt DNA gave a ratio of UV absorbance more than 1.8 at 260 and 280 nm, indicating that DNA was sufficiently free from protein [14]. The stock solution of FM-DNA was prepared by dissolving DNA in 10mM of the Tris–HCl buffer at pH 7.0. The DNA concentration of the stock solution was determined by UV spectrophotometery, in properly diluted samples, using the molar absorption coefficient 6600 $M^{-1}.cm^{-1}$ at 260 nm [15]. The stock solutions were stored at 4^{o}C and used over no more than 4 days. Absorption titration experiments were performed with fixed concentration of the complexes ($1x10^{-3}$M) while gradually increasing the concentration of DNA ($0.5–8x10^{-4}$M) at 25^{o}C. While measuring the absorption spectra, an equal amount of DNA was added to both the compound solution and the reference. To compare quantitatively the affinity of the compound bound to DNA by the luminescence titration method, fixed amounts of the complexes ($1x10^{-4}$M) were titrated with increasing amounts of DNA at 25^{o}C, over a range of DNA concentrations from 5 to 80 μM.

3.Results and discussion

3.1.Ligand characterization

The Schiff-bases H_2L^1, H_2L^2, H_2L^3, H_2L^4 and H_2L^5 were obtained by condensation of lysine with the corresponding aldehyde (1:1) in ethanolic medium [12]. Schiff-bases of lysine with phthaldehyde [9] and o-vaniline [11] were also obtained with 1:1 ratio by the same method. We were able to isolate salicylaldenelysine Schiff-base which was stable for 24h through which we obtained its IR and ^{1}H NMR spectra. Free lysine presents as an inner salt $H_3N^+(CH_2)_4–CH(NH_2)COO^-$, its IR spectrum shows (NH3+) and (COO^-) characteristic absorption peaks. The IR spectrum of the free salicylaldenelysine Schiff-base shows two medium sharp bands at 3163 and 2937 cm-1 assigned to the asymmetric and symmetric stretching vibration of $NH3^+$. This indicates that the condensation reaction only occurred between salicylaldehyde and α–NH_2 of lysine, while ε–NH_2 remained unchanged [16]. The ligand exhibits one sharp band at 1615 cm^{-1} due to the azomethine stretching vibration. It displays characteristic IR spectral bands at 1583 and 1350 cm^{-1} that are assignable to $\upsilon_{as}(COO^-)$ and $\upsilon_{sym}(COO^-)$ moiety [17]. Infrared absorption curve for the solid Schiff-base shows a medium width band at 3400 cm^{-1} due to mole of crystal water retained in most of the hydroxyl-aldehyde Schiff-bases [18]. Based on the above mentioned data, the Schiff-base has structure **1**. ^{1}H NMR spectrum of the salicylaldenelysine Schiff-base in DMSO-d_6 shows signal at δ 8.53 ppm due to –CH=N proton which confirms the formation of the ligand. Aromatic protons resonate as multisignals at δ 6.82-7.41 ppm. δ_H >10 ppm is not observed at the downfield, meaning that proton in hydroxybenzene group is absent, which is consistent with the IR analysis. These data show that H_2L^1-H_2L^5 Schiff-bases are functioning as bivalent tridentate ligand.

3.2.Nickel(II) complexes

The nickel(II) complexes of the Schiff-bases H_2L^1-H_2L^5 are stable in air, soluble in strong polar organic solvents such as DMSO and DMF. The molar conductance values of 10^{-3}M DMSO solutions (Table 1) suggest the complexes to be non-electrolytes [19]. Elemental analysis show that the composition of the complexes are in agreement with the formulation of $[Ni(L^{1,5})X_m].nH_2O$ where X = H_2O; m = 3, 1; n = 2½, 1 or X = NH_3; m = 1; n = 1; $[NiL^{2,3,4}(H_2O)_3].2½H_2O$ and $[Ni(HL^{2,3,4})(NH_3)(H_2O)_2].nH_2O$ where n = 2½ , 3, 3.

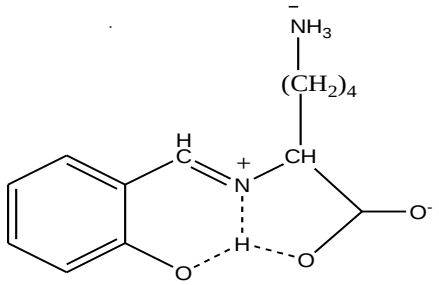

Structure 1: Salicylaldenelysine Schiff-base.

Table 1: Analytical data, conductivity and magnetic moments of the nickel(II) complexes of the lysine Schiff-bases.

Compound	Color	Mol. Wt.	Melting & Dec. Point °C	Elemental analysis Found Calcd.%				Ω*	μ_{eff} B.M.
				C	H%	N%	M%		
[NiL1(H2O)3].2½H2O	Bluish green	405.98	>385	38.7 38.4	3.6 3.9	6.4 6.7	13.9 14.5	25	3.23
$[NiL^1(NH_3)].H_2O$	Reddish brown	341.98	335-338	45.5 45.6	4.9 4.8	8.4 8.2	17.7 17.2	14	Dia
$Ni(HL^2)(H_2O)_3].2½H_2O$	Olive	422.98	>380	36.6 36.8	3.6 3.9	6.3 6.6	13.5 13.9	36	3.51
$[Ni(HL^2)(NH_3)(H_2O)_2].2½H_2O$	Deep brown	420.98	>375	36.7 36.9	3.8 4.0	6.6 6.7	13.7 13.9	19	3.29
$[Ni(HL^3)(H_2O)_3].2½H_2O$	Olive	421.98	>385	37.1 36.9	3.6 3.9	6.7 6.6	13.7 13.9	38	3.48
[Ni(HL3)(NH3)(H2O)2].3H2O	Deep brown	429.98	>390	36.5 36.3	3.6 3.8	6.6 6.2	13.6 13.7	20	3.43
[Ni(HL4)(H2O)3].2½H2O	Gray	421.98	>370	37.3 36.9	3.6 3.9	6.3 6.6	13.5 13.9	35	3.37
[Ni(HL4)(NH3)(H2O)2].3H2O	Deep Olive	429.98	>380	36.7 36.3	3.6 3.9	7.6 6.5	13.4 13.7	13	3.04
[NiL5(H2O)].H2O	Straw yellow	392.03	>385	52.3 52.0	4.5 4.7	6.5 6.9	14.5 14.97	21	1.84
[NiL5(NH3)].H2O	Reddish brown	391.03	>375	52.7 52.1	4.6 4.8	7.3 7.1	14.6 14.97	14	2.39

*10^{-3}M in DMSO, $ohm^{-1}.cm^2.mol^{-1}$.

3.2.1. *IR spectra*

The selected IR spectra of the nickel(II) complexes along with their tentative assignments are reported in Table 2. The IR spectra of the complexes show the presence of absorption bands at 3116-3046 and 3015-2926 cm^{-1} which indicates the non-participation of the ε–NH_2 group in complex formation [7]. A very strong broad band is resolved into two components at 1641-1616 and 1610-1570 cm^{-1} assigned to the C=N absorption frequency and the superposition of $\upsilon_{as}(COO^-)$, υ(C=C) and υ(C=N). Also, a new absorption band, assigned to the $\upsilon_{sym}(COO^-)$ vibration, appears at 1388-1313 cm^{-1}. $|\upsilon_{as} - \upsilon_{sym}|$ of the carboxylic group ranges from 280 to 168 cm^{-1} which shows that it is coordinated as unidentate ligand [20]. A medium strong band at 1578-1529 cm^{-1}, always present, may originate from the vibration of (Ph-C-C=N) band and typifies complexes derived from salicylaldehyde or naphthaldehyde [21]. Nickel(II) complexes with ligands H_2L^2-H_2L^4 show υOH of the second hydroxyl group at 3305-3218 cm^{-1} indicating non-coordination to the Ni(II) ion. Coordinated ammonia shows υ(NH) as strong sharp band at 3302, 3171, 3156, 3171 and 3319 cm^{-1}, respectively. Medium strong band at 1286-1223 cm^{-1} may corresponds to υ(Ph–O) frequency. The broad band at 3426-3356 cm^{-1} may be assigned as stretching due to the presence of crystallization water. The new peaks appearing between 605-546 and 504-437 cm^{-1} are assigned to υ(Ni-O) and υ(Ni-N). This is additional confirmation of the involvement of the coordination of nitrogen and oxygen to the nickel(II) ion [22].

Table 2: IR spectral data of the nickel(II) complexes of the lysine Schiff-bases

Compound	$\upsilon(H_2O)$	υ(OH)	υ(NH)	υ(C=N)+ $\upsilon_{as}(COO^-)$	υ(Ph-C-C=N)	$\upsilon_{sym}(COO^-)$	$\Delta\upsilon$	υ(C-O)	υ(M-O)	υ(M-N)
H_2L^1 $C_{13}H_{17}O_3N_2Na.H_2O$	3400b	–	3163m 2937sh	1615┐ s 1583┘	1562m	1350m	–	–	–	–
$[NiL^1(H_2O)_3].2½H_2O$	3420b	–	3054m 2926m	1641┐ s 1608┘	1531m	1328m	280	1279m	548m	451m
$[NiL^1(NH_3)].H_2O$	3426b	–	3302s 3060m 3015m	1617┐ s 1570┘	1529s	1328m	242	1259m	595m	466m
$[NiL^2(H_2O)_3].2½H_2O$	3391b	3305sh	3070b 2929m	1639┐ s 1609┘	1578m	1385m	224	1246m	559m	490m
$[NiL^2(NH_3)(H_2O)_2].2½H_2O$	3379b	3234b	3171b 3046sh 2929m	1632┐ s 1578┘	1546m	1313m	265	1235m	546m	485m
$[NiL^3(H_2O)_3].2½H_2O$	3382b	3296m	3116b 2945m	1640┐ s 1608┘	1546s	1328m	280	1224m	549m	504m
$[NiL^3(NH_3)(H_2O)_2].3H_2O$	3356b	3218b	3156b 3062b 2931m	1637┐ s 1600┘	1552s	1380m	220	1223m	605m	495m
$[NiL^4(H_2O)_3].2½H_2O$	3382b	3234b	3054b 2946m	1640┐ s 1580┘	1550s	1382m	198	1285m	555m	500m
$[NiL^4(NH_3)(H_2O)_2].3H_2O$	3360b	3250b	3171b 3060b 2928m	1636┐ s 1581┘	1550s	1388m	193	1286m	560m	492m
$[NiL^5(H_2O)].H_2O$	3420b	–	3059m 2927m	1630┐ s 1610┘	1544m	1358m	168	1283m	570m	502m
$[NiL^5(NH_3)].H_2O$	3423b	–	3319m 3052m 2926m	1616┐ s 1600┘	1534m	1354m	260	1276m	550m	437m

sh = sharp, s = strong, b = broad, m = medium

3.2.2.Magnetic and UV-Vis spectral properties

Electronic spectral data and magnetic moments give information regarding geometry of the Ni(II) complexes (Table 3). Diamagnetism of the complex $[NiL^1(NH_3)].H_2O$ indicates its square planner geometry. Its electronic spectrum shows absorption band at 566 nm (nujol mull) due to $^1A_{2g}\leftarrow{}^1A_{1g}(\upsilon_1)$ transition of square planner structure. Absence of any transitions at longer wavelength confirms this geometry indicating a large crystal field splitting [23]. Anomalous magnetic moment of the complexes $[NiL^5(H_2O)].H_2O$ and $[NiL^5(NH_3)].H_2O$ may result from either spin-spin coupling [24] or configurational equilibrium [25] which is indirectly suggested by the low observed magnetic moment although we do not have a direct evidence for its existence. By assuming an equilibrium between paramagnetic octahedral (a value of 3.2 B.M. is the average of magnetic moments of Ni(II) complexes of salicylideneaminoacid [26]) and diamagnetic square planar configuration, it can be calculated that the ratio of square planar : octahedral type is approximately 33% and 56% for both complexes. Rest of the complexes have magnetic moment in the 3.51-3.04 B.M. range which indicates octahedral geometry around the Ni(II) ion [27]. The electronic spectra of these complexes (DMSO) show d-d bands at 750-739 and 684-672 nm. These are assigned to the spin-allowed transitions $^3T_{2g}(F)\leftarrow{}^3A_{2g}(F)(\upsilon_1)$ and $^3T_{1g}(F)\leftarrow{}^3A_{2g}(F)(\upsilon_2)$ consistent with their well-defined octahedral configuration [28]. Absorption bands at 440-384 nm (nujol mull) and 443-370 nm (DMSO) for all complexes were assigned to metal→ligand charge transfer.

Table 3: Electronic spectra of the nickel(II) complexes of the lysine Schiff-bases.

Compound	Nujol mull (nm)				DMSO (nm)			
	π→π*	n→π*	CT	d→d	π→π*	n→π*	CT	d→d
$[NiL^1(H_2O)_3].2½H_2O$	270	321 347 366	384	−	253 258	300	381	675 745
$[NiL^1(NH_3)].H_2O$	260 275	324 339 364	431	566	264 270	322 338	404	−
$[NiL^2(H_2O)_3].2½H_2O$	275	315 342 364	408	−	273	303 327	384 418	675 743
$[NiL^2(NH_3)(H_2O)_2].2½H_2O$	270	320 356 360	430	−	274	305 327	384 417	673 740
$[NiL^3(H_2O)_3].2½H_2O$	275	316 345 366	440	−	279	317 353	383 418	684 750
$[NiL^3(NH_3)(H_2O)_2].3H_2O$	260 270	319 352 364	440	−	257 279	322 354	−	683 750
$[NiL^4(H_2O)_3].2½H_2O$	275	324 358 367	440	−	263 272	304 325	454	684 746
$[NiL^4(NH_3)(H_2O)_2].3H_2O$	275	317 345 366	385 430	555	263 271	309 349	370 430	672 739
$[NiL^5(H_2O)].H_2O$	275	320 342 368	430	−	263 269	311 350	395 413 443	−
$[NiL^5(NH_3)].H_2O$	280	316 340 368	436	527	274 279	311 331 354	417 442	−

3.2.3.^{1}H NMR spectra

1H NMR spectrum of the complex [NiL1(NH3)].H2O in DMSO-d6 is shown in Figure 1. 1H nmr data of the complex show that it resonates at δ 3.46 ppm due to –CH– proton of the lysine moiety. –CH2– groups of the lysine resonate at δ 1.03, 1.07, 1.1 and 2.5 ppm, respectively. Protons of the aromatic ring resonate in two groups at δ 6.47-6.8 and 7.11-7.35 ppm. The signals of the H atom of the azomethine group are observed as a doublet at δ 7.51 and 7.8 ppm. This high field shift is assigned to the increase of the shielding effect due to decrease of the electron cloud density of H atom at α-CH group after coordination with the nickel(II) ion [9]. Splitting of the azomethine signal was observed with isostructural Schiff-bases [29-31] and suggests the presence of proton transfer equilibrium and the existence of NH tautomer in the studied compounds. This is confirmed by the spectrum in D_2O which shows the azomethine proton as a singlet due to the deutration of the NH

tautomer. A broad signal is observed at δ 8.58 ppm, exchangeable with D_2O, may be assigned to the presence of the NH_3 co-ligand or due to the bonded phenolic OH group. According to the above mentioned data, the ligands (H_2L^1- H_2L^5) behave as dibasic tridentate towards nickel(II) ions, via two deprotonated oxygen atoms, one of each of the salicylaldehyde and carboxylic acid moieties, and nitrogen atom of the azomethine-N, forming 5- and 6-membered stable chelate rings around the central metal ion thus giving overall constancy to the nickel(II) complexes.

3.2.4.Thermal analysis

The nickel(II) complexes were subjected to TG-DTA analysis from ambient temperature up to 750°C in nitrogen atmosphere. The temperature ranges, percentage mass losses and thermal effects accompanying the decomposition are given in Tables 4, 5. Representative thermal curves TG/DTG-DTA of the nickel complexes are given in Figure 2. For all the investigated complexes, the thermal decomposition mode in nitrogen seems to follow the same model. The first decomposition step includes the elimination of crystallization water at 55-79°C and evolution of 1, 2½ and 3 water molecules, respectively, associated with endothermic DTA peaks at 60-85°C indicating non-coordinated waters and they are hydrated water. For all the investigated complexes, the thermal decomposition mode in nitrogen seems to follow the same model.

Fig. 1: ^{1}H nmr spectrum of $[NiL^1(NH_3)].H_2O$

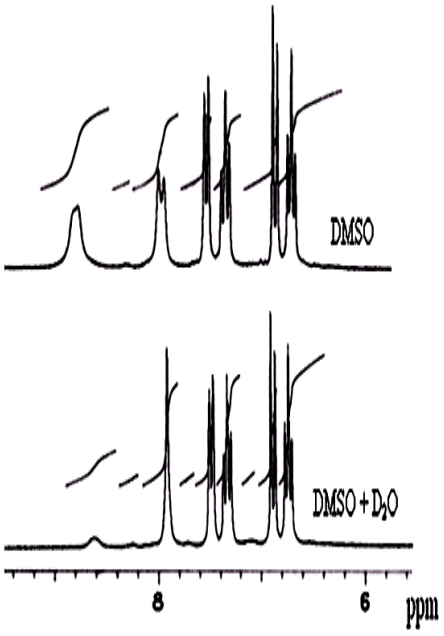

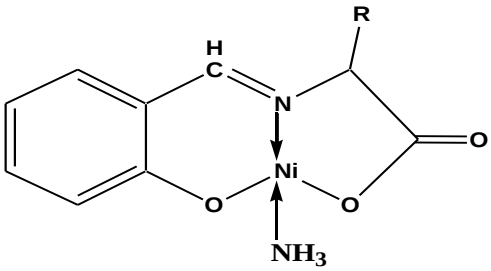

Square planar structure

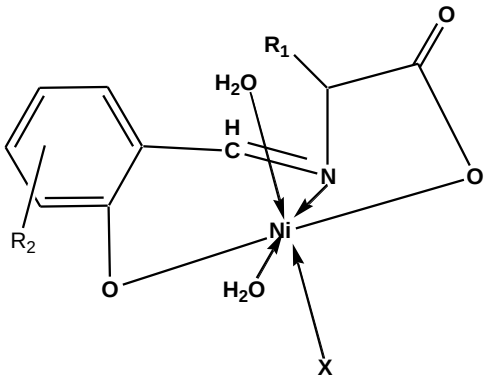

Octahedral structure
X=H2O or NH3
R1= -(CH2)4 - NH2
R2 = H, o-OH, m-OH or p-OH

Structure 2: Ni(II) complexes of the lysine Schiff-bases.

The first decomposition step includes the elimination of crystallization water at 55-79°C and evolution of 1, 2½ and 3 water molecules, respectively, associated with endothermic DTA peaks at 60-85°C indicating non-coordinated waters and they are hydrated water. Pyrolytic decomposition of the anhydrous complexes takes place in the second decomposition step which concerns about dissociation of the coordination sphere. In the second decomposition stage, coordinated water of $[NiL^1(H_2O)_3].2½H_2O$ is removed at 302°C with mass loss of 13.0% (calcd. 13.3%) associated with exothermic DTA peak at 302°C. In the same stage, $[NiL^2(NH_3)(H_2O)_2].2½H_2O$, $[NiL^3(NH_3)(H_2O)_2].3H_2O$ and $[NiL^4(NH_3)(H_2O)_2].3H_2O$ lose ammonia, water and $H_2N–C_2H_5$ species at 297, 341 and 320°C, respectively. The observed mass loss was: (found/calcd.%) 22.79/23.33%, 22.22/22.84% and 23.22/22.84% associated with exothermic DTA peaks at 297, 341 and 321°C, respectively. Also,

$[NiL^1(NH_3)].H_2O$, $[NiL^2(H_2O)_3].2½H_2O$ and $[NiL^5(NH_3)].H_2O$ lose NH_3 or H_2O in addition to H_2N-C_5H_{11} and H_2N-C_3H_7 species at 331, 340 and 353°C, respectively. This step was confirmed by the presence of exothermic DTA maxima at 333, 335 and 357°C showing weight loss of 31.0, 33.64 and 19.15 % (calcd. 30.41, 33.41 and 19.38%), respectively. The third decomposition step concerns with degradation of the Schiff-bases which takes place at 370, 405; 463; 416, 546; 447; 448, 655; 463 and 392°C, respectively, for the previously discussed complexes. Broad exothermic DTA peaks at 370, 405; 472; 452, 512; 463; 461, 484; 460 and 357, 396oC, respectively, confirm this step. Coordination sphere of the complex $[NiL^5(H_2O)].H_2O$ dissociates in two steps. In the first one, the complex loses one molecule of coordinated water and the fragment C_6H_6+H_2N-$(CH_2)_4$-COOH and rest of the Schiff-base evolves in the second one. The complexes $[NiL^3(H_2O)_3].2½H_2O$ and $[NiL^4(H_2O)_3].2½H_2O$ behave differently where the coordination sphere decomposes completely in one step extending in the 200- 665 and 200-697°C range with DTG maxima at 482 and 423°C associated with broad exothermic DTA peaks at 484 and 421°C. NiO is obtained as a result of the final decomposition stage.

Fig. 2: TG, DTG and DTA analysis of $[NiL^5(H_2O)].H_2O$.

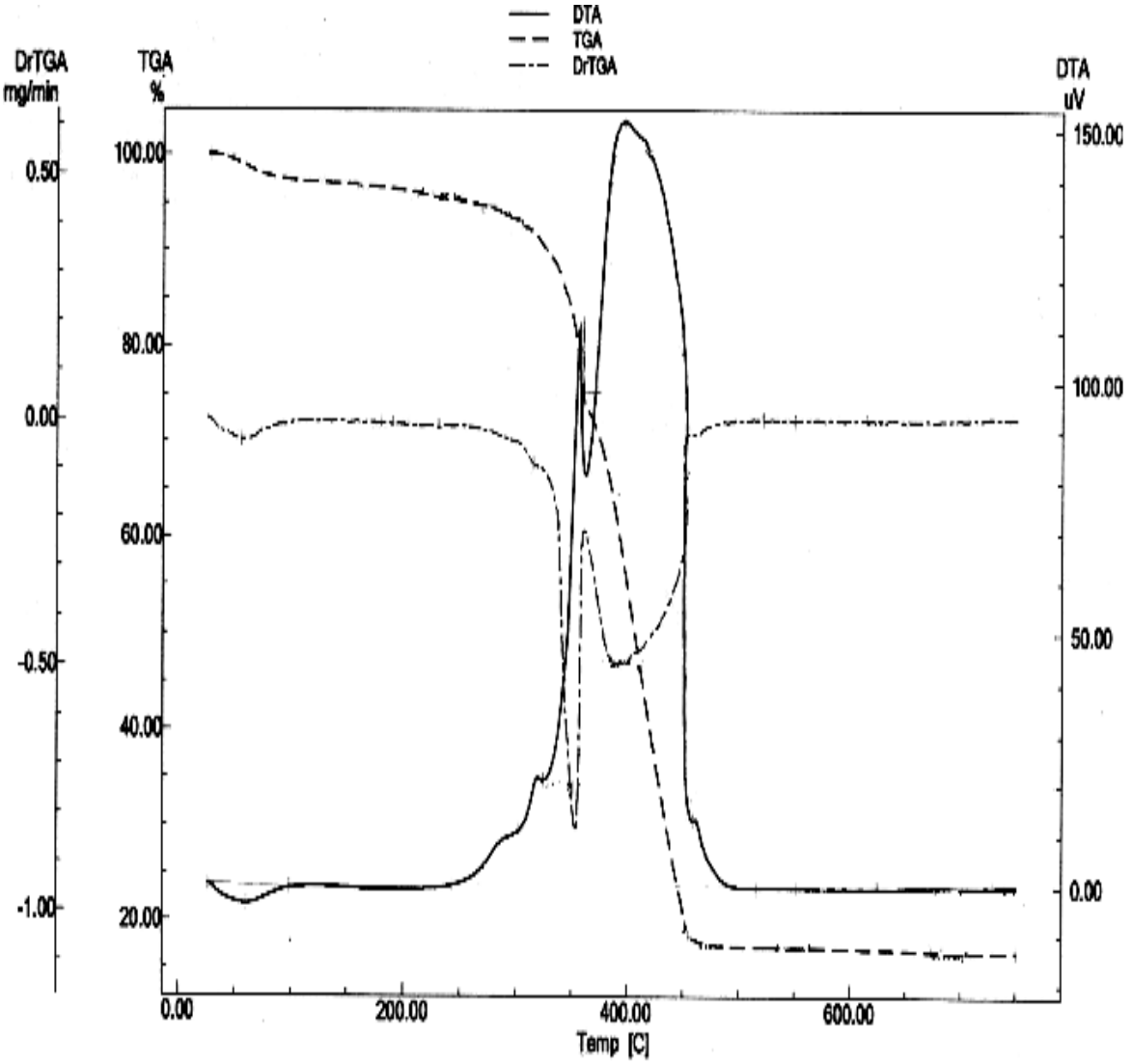

Table 4: TGA and DTG of the nickel(II) complexes of the lysine Schiff-bases

Residue	Expected products	Process	Mass loss %		DTG tem. °C	Tem. rang °C	Compound
Found (Calcd.)%			Calcd.	Found			
NiO 20.0 (18.4)	2½H_2O 3 H_2O H_2N-$(CH_2)_5$-COOH 0.42 L	Dehydration Coordination sphere Ligand decomposition Final decomposition	11.1 13.3 32.26 25.89	10.44 13.0 32.23 24.15	70 302 370┐ 405┘ 490	34-125 220-320 340-420 440-569	$[NiL^1(H_2O)_3].2½H_2O$
NiO 22.22 (21.84)	H_2O NH_3 + H_2N-C_5H_{11} 0.6 L	Dehydration Coordination sphere Ligand decomposition Final decomposition	5.26 30.41 42.45	4.5 31.0 42.28	55 331 448┐ 655┘	41-169 211-388 405-727	$[NiL^1(NH_3)].H_2O$
NiO 19.16 (17.69)	2½H_2O 3 H_2O + H_2N-C_5H_{11} 0.77 L	Dehydration Coordination sphere Final decomposition	10.63 33.41 37.86	10.50 33.64 36.5	78 340 463	44-150 200-390 410-520	$[NiL^2(H_2O)_3].2½H_2O$
NiO 16.11 (17.7)	2½H_2O NH_3+2H_2O+H_2N-C_2H_5 0.8L	Dehydration Coordination sphere Final decomposition	10.71 23.33 48.71	10.56 22.97 50.56	75 297 463	55-120 180-320 325-525	$[NiL^2(NH_3)(H_2O)_2].2½H_2O$
NiO 16.99 (17.7)	2½H_2O 3 H_2O + 0.94L	Dehydration Coordination sphere	10.66 72.12	9.72 73.61	68 482	35-150 200-665	$[NiL^3(H_2O)_3].2½H_2O$
NiO 17.22 (17.4)	3 H_2O NH_3+2H_2O +H_2N-C_2H_5 0.21 L 0.56 L	Dehydration Coordination sphere Ligand decomposition Final decomposition	12.56 22.79 13.01 34.68	11.67 22.22 13.00 35.88	73 341 416┐ 546┘	35-130 200-350 370-610	$[NiL^3(NH_3)(H_2O)_2].3H_2O$

http://www.aun.edu.eg

E-mail: president@aun.edu.eg

Compound	Temp. range ^{o}C	DTA temp. ^{o}C	ΔH (J/g)	Process
$[NiL^{1}(H_2O)_3].2½H_2O$	29-150 254-320 330-430 450-575	76 exo. 302 exo. 373┐ exo. 408┘ 492 exo.	-489 -10140	Dehydration Coordination sphere Ligand decomposition Final decomposition
$[NiL^{1}(NH_3)].H_2O$	44-146 251-384 400-585 600-688	85 endo. 318┐ exo. 333┘ endo. 461┐ exo. 484┘ 656 endo.	41 -202 104 -2270 333	Dehydration Lattice rearrangement Melting Coordination sphere Ligand decomposition Solid state reaction.
$[NiL^{2}(H_2O)_3].2½H_2O$	25-169 193-350 360-622	82 endo. 335 exo. 46	657 -10650	Dehydration Coordination sphere Final decomposition
$[NiL^{2}(NH_3)(H_2O)_2].2½H_2O$	26-171 201-392 402-546	79 endo. 297 exo. 472 exo.	617 -2100 -7100	Dehydration Coordination sphere Final decomposition
$[NiL^{3}(H_2O)_3].2½H_2O$	31-143 245-682	75 endo. 484 exo.	480 -9030	Dehydration Coordination sphere
$[NiL^{3}(NH_3)(H_2O)_2].3H_2O$	33-148 274-360 374-603	80 endo. 341 exo. 425┐ exo. 512┘	498 -1900	Dehydration Coordination sphere Ligand decomposition Final decomposition
$[NiL^{4}(H_2O)_3].2½H_2O$	34-174 203-710	82 endo. 421 exo.	576 -8780	Dehydration Coordination sphere
$[NiL^{4}(NH_3)(H_2O)_2].3H_2O$	35-168 201-374 374-523	83 endo. 321 exo. 463 exo.	601 -3070 -7850	Dehydration Coordination sphere Ligand decomposition
$[NiL^{5}(H_2O)].H_2O$	33-131 300-370 412-717	72 endo. 328 exo. 466 exo.	262 -18 -1670	Dehydration Coordination sphere Final decomposition
$[NiL^{5}(NH_3)].H_2O$	26-98 243-496	60 endo. 357┐ exo. 396┘	134 -13450	Dehydration Coordination sphere Final decomposition

3.2.5.Mechanism of thermal decomposition

Elucidation of thermal decomposition mechanism is obtained by tracing IR spectra for heated samples of the complexes at different temperatures. Accordingly, samples of the complexes $[NiL^{1}(H_2O)_3].2½H_2O$ and $[Ni(HL^{2})(NH_3)(H_2O)_2].2½H_2O$ were heated at 200, 400 and 540^{o}C, respectively, and their IR spectra are shown in Figure 3. Heated samples at 200^{o}C show IR spectra of no difference compared to that obtained at room temperature indicating dehydration [30]. IR spectra of heated of the complexes at 400^{o}C show the disappearance of $\upsilon_{as}(COO^{-})$, $\upsilon_{sym}(COO^{-})$, υ(C=N) and υ(NH) of ammonia coligand which indicates the decomposition inside the coordination sphere.

In the same time, appearance of new medium sharp band at 2360 and 2335 cm^{-1} which may be assigned to formation of –C≡N group [30]. In the same time, preservation of distinctive bands at 2922 and 2933 cm^{-1} assigned to υ(CH_2), 1051 and 1060 cm^{-1} of δ(CH_2) are observed. The appearance of bands characteristic to aqua-hydroxo complexes corresponding to υ(OH) at 3391 and 3438 $cm^{-1}$and δ(OH) at 1600 and 1620 cm^{-1} were remarkable [32]. Final decomposition of the complexes at 540°C show υ(Ni–O) of the NiO as s final product at 429 and 430 cm^{-1} [33]. Mechanism of the thermal decomposition for the complex $[NiL^1(H_2O)_3].2½H_2O$ is represented as follows:

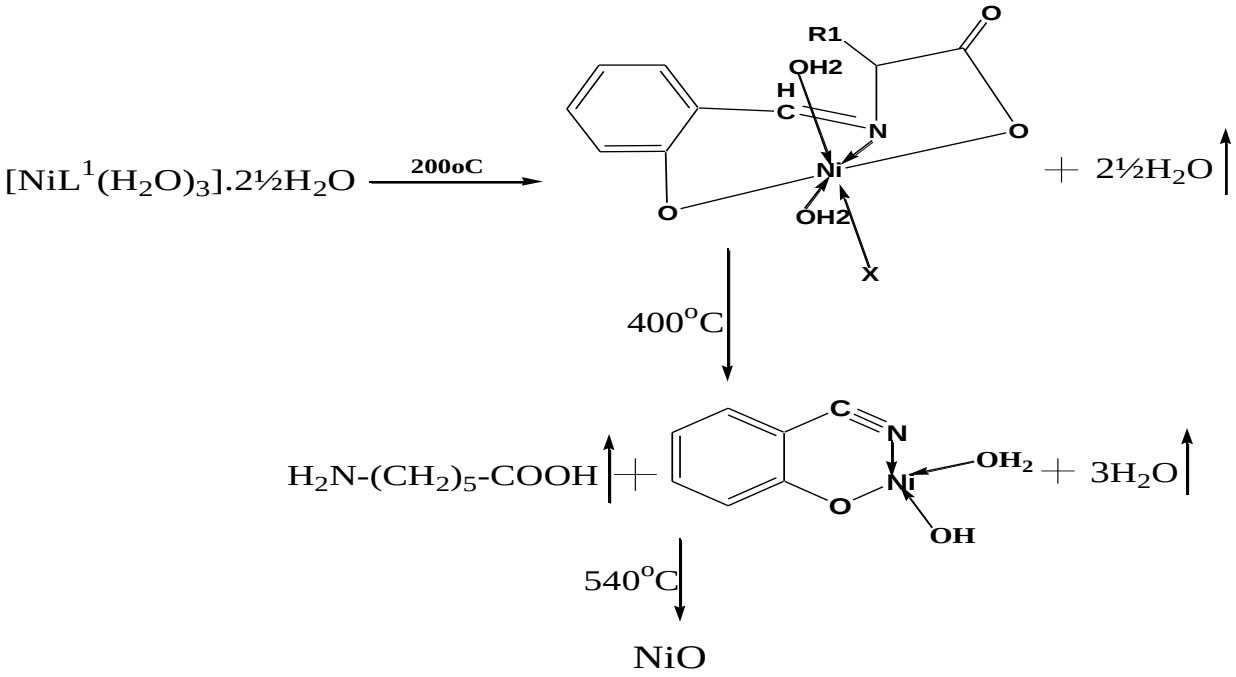

Fig. 3: IR spectrum of $[NiL^1(NH_3)].H_2O$ at different temperatures.

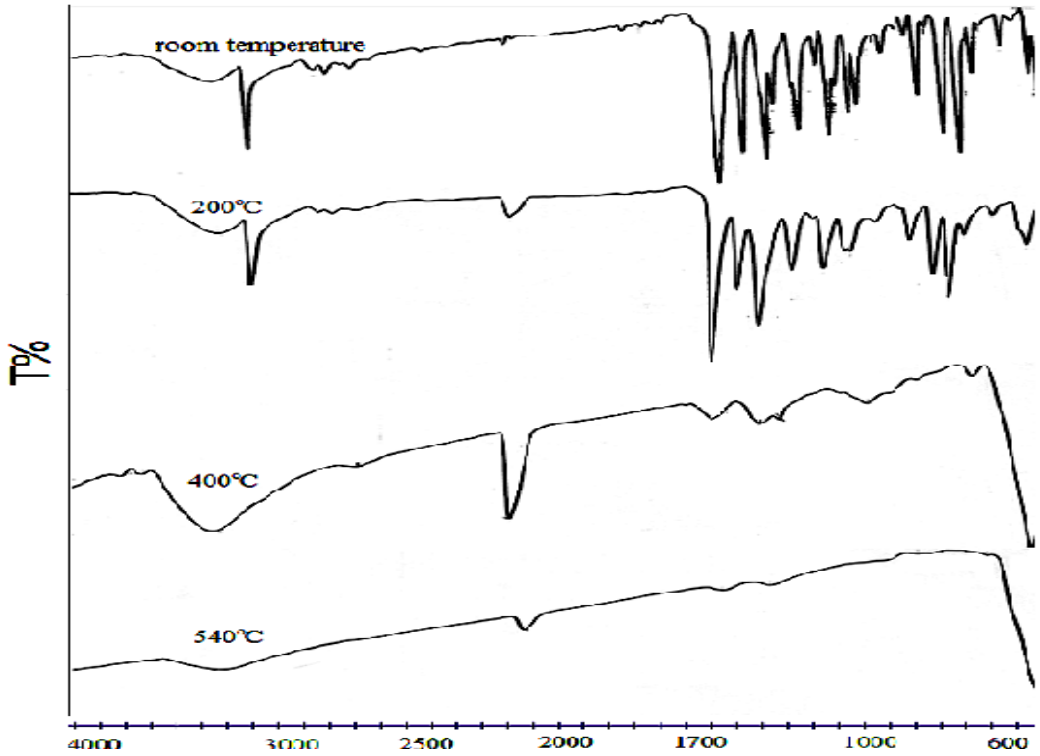

Table 6: Kinetic parameters for the decomposition steps of the nickel(II)complexes of the lysine Schiff-bases.

Compound		Order n	T_s K^o	ΔE_a [b]	Z [c]	ΔS [d]	ΔH [b]	ΔG [b]
$[NiL^1(H_2O)_3].2½H_2O$	I	0.5	348	0	0.6	-97	27	34
	II	0	579	92	21	-72	87	42
$[NiL^1(NH_3)]\ H_2O$	II	0	603	92	19	-73	87	44
$[NiL^2(H_2O)_3].2½H_2O$	I	2	353	70	0.3	-104	67	37
	II	0.5	614	49	2.5	-90	44	55
$[NiL^2(NH_3)(H_2O)_2].2½H_2O$	I	2	353	82	0.4	-100	79	36
	II	0	581	37	3	-88	32	51
$[NiL^3(H_2O)_3].2½H_2O$	I	0	342	80	0.5	-99	77	34
$[NiL^3(NH_3)(H_2O)_2].3H_2O$	I	2	348	87	0.5	-100	84	35
$[NiL^4(H_2O)_3].2½H_2O$	I	2	350	90	0.2	-105	86	37
$[NiL^4(NH_3)(H_2O)_2].3H_2O$	I	0	361	35	1.3	-92	32	33
$[NiL^5(H_2O)].H_2O$	I	2	342	90	0.7	-96	87	33
	II	0	598	41	3.3	-88	36	52
$[NiL^5(NH_3)].H_2O$	I	0	628	77	2 0	-73	71	46
	II	0	675	41	3.3	-89	35	60

[b] kJ/mol
[c] values x 10^8 ; S^{-1}
[d] kJ/mol. K

3.2.6.Kinetic parameters

For the kinetic analysis of individual steps of isolated complexes, we applied Coates-Redfern method using TG and DTG curves [34]. The degradation steps with no well resolved TG curves were not suitable and consequently were not the objective of this analysis. The order (n), the pre-exponential factor (Z) and the heat of activation ΔE_a of the various decomposition stages were determined. The other kinetic parameters ΔH, ΔS and ΔG were also computed and values are presented in Table 6. The following remarks can be obtained:

1. The negative values of the activation entropies ΔS indicate more ordered activated complexes than the reactants and/or the reactions are slow [35].

2. There are no obvious trends in the values of the heat of activation ΔE_a or the activation enthalpies ΔH. however, the values of activation free energy ΔG increases significantly for the subsequent decomposition stages for a given complex. This is due to increasing the values of $T\Delta S$ from one step to another which override the values of ΔH.

3. Values of activation energy and activation enthalpy of dehydration process of the isostructureal complexes $[NiL^2(H_2O)_3].2½H_2O$, $[NiHL^3(H_2O)_3].2½H_2O$ and $[NiL^4(H_2O)_3].2½H_2O$ are: ΔE_a: 70<80<90; ΔH: 67<77<86. Increase of ΔE_a and ΔH values of these complexes may correlate to the structure of H_2L^2, H_2L^3 and H_2L^4 where they contain a second o-, m- and p-OH group capable of strongly hydrogen bonding. This order reflects the backing structure which may allow stronger interactions of lattice water molecules in crystals.

3.3.DNA interaction

Assuming that DNA forms a 1:1 complexes with Ni(II)-complexes, the binding constant of the formed complexes (K_b) is given by Benesi–Hildebrand plot [47]:

$$\frac{[Ni-complex]_o}{\Delta A} = \frac{1}{\Delta \varepsilon} + \frac{1}{K\,\Delta \varepsilon\,[DNA]_o}$$

Where, ΔA is the difference between the

absorbance of Ni(II)-complex in presence and absence of DNA, Δε is the difference between the molar absorption coefficients of Ni(II)- complex and Ni(II)-complex-DNA systems. $[Ni(II)\text{-complex}]_o$ and $[DNA]_o$ are the initial concentration of Ni(II)-complex and DNA. Linear relationship of $[Ni(II)\text{-complex}]_o$ /ΔA *vs.* $1/[DNA]_o$ confirms the formation of a 1:1 Ni(II)-complex-DNA system. from its intercept and slope values, K_b is evaluated at room temperature. The change of emission intensity in emission titrations ensured the availability of the association constants (K) of the complexes with DNA from the analysis of the relationship between the fluorescence intensity and the DNA by Benesi–Hildebrand plot [47]. The association constants of the formed complexes (K) are given by:

$$\frac{I_{F_o}}{I_F - I_{F_o}} = \alpha + \frac{\alpha}{K[DNA]_o} \quad , \quad \alpha = \frac{1}{I_{F_L} - I_{F_o}}$$

Where $[DNA]_o$ represents the analytical concentration of DNA, I_{Fo} and I_F are the fluorescence intensities in the absence and presence of DNA and I_{FL} is the limiting intensity of fluorescence and α is $1/(I_{FL} - I_{Fo})$. A plot of $I_{Fo}/(I_F - I_{Fo})$ *vs.* $1/[DNA]_o$ should give a straight line with a good linear relationship.

3.3.1.Electronic absorption titration

The absorption spectra of the complexes of Ni(II)-lysine Schiff-bases in presence of FM-DNA (at a constant concentration of the complex) are given in Figure 4 and Table 7.

The potential FM-DNA binding ability of the complexes was studied by following the intensity changes of the intraligand π–π* transition bands in the uv. spectra [48]. In presence of DNA, the absorption bands of the complexes at about 254-275 nm exhibited hyperchromism of about 15-97% and blue shift of about 7-9 nm. Therefore, the observed hyperchromism reflect strong structural damage, which is probably due to strong binding of the complexes to the DNA base moieties through covalent-bond formation [49]. The intrinsic binding constants K_b of the complexes were in the $2.3x10^4$ – $6.4x10^4$ M^{-1} range. The values indicate that the nickel(II) complexes are moderately bind to FM-DNA with almost the same affinity. However, these values are smaller than those of classical intercalators whose K_b values are in order of 10^7M^{-1} [50]. Therefore, it is likely that the proposed covalent binding of the complexes is more feasible although electrostatic interactions can not be ruled out.

Table 7: Binding constant (K M-1) of the interaction between Ni(II) complexes of the lysine Schiff-bases and FM-DNA.

compound	U.V.			Fluorescence		
	K_b M^{-1}	Hyper. %	Δ/λ	K M^{-1}	Hyper. %	Δ/λ
$[NiL^1(H_2O)_3].2½H_2O$	$2.8\ x10^4$	21	–	$2.2\ x10^4$	19	–
$[NiL^1(NH_3)].H_2O$	$2.3\ x10^4$	22	–	$4.8\ x10^4$	56	-52
$[NiL^2(H_2O)_3].2½H_2O$	$3.5\ x10^4$	55	-7	$7.1\ x10^4$	42	–
$[NiL^2(NH_3)(H_2O)_2].2½H_2O$	$3.8\ x10^4$	43	-7	$2.4\ x10^4$	57	–
$[NiL^3(H_2O)_3].2½H_2O$	$2.4\ x10^4$	18	–	$1.9\ x10^4$	39	-17
$[NiL^3(NH_3)(H_2O)_2].3H_2O$	$2.7\ x10^4$	15	–	$1.0\ x10^4$	51	+9
$[NiL^4(H_2O)_3].2½H_2O$	$6.4\ x10^4$	97	–	$7.3\ x10^4$	50	–
$[NiL^4(NH_3)(H_2O)_2].3H_2O$	$4.6\ x10^4$	68	-10	$7.8\ x10^4$	69	–
$[NiL^5(H_2O)].H_2O$	$2.3\ x10^4$	74	–	$3.9\ x10^4$	21	–
$[NiL^5(NH_3)].H_2O$	$3.1\ x10^4$	69	–	$3.1\ x10^4$	30	–

3.3.2Fluorescence titration studies

The nickel(II) complexes under study can emit fluorescence in Tris-HCl buffer at ambient temperature with maxima appearing at about 339-848 nm. As shown in Figure 5, the fluorescence intensities of the complexes are increased steadily with increasing concentration of FM-DNA, which agrees with those observed for other intercalators [51] and indicate their interaction with FM-DNA.

This implies that the complexes can insert between DNA base pairs deeply and that they can bind to DNA. The binding of the complexes to DNA leads to a marked increase in emission intensity which is also observed with complexes containing a ligand bearing NH and OH groups [52,53]. The evaluated association constant (K) evaluated are in the 1.0-7.8x10^4 M^{-1} range.

Fig. 5: The emission enhancement spectra of [NiL1(NH3)].H2O (10-4M) in presence of 0 – 80 μM FM-DNA.

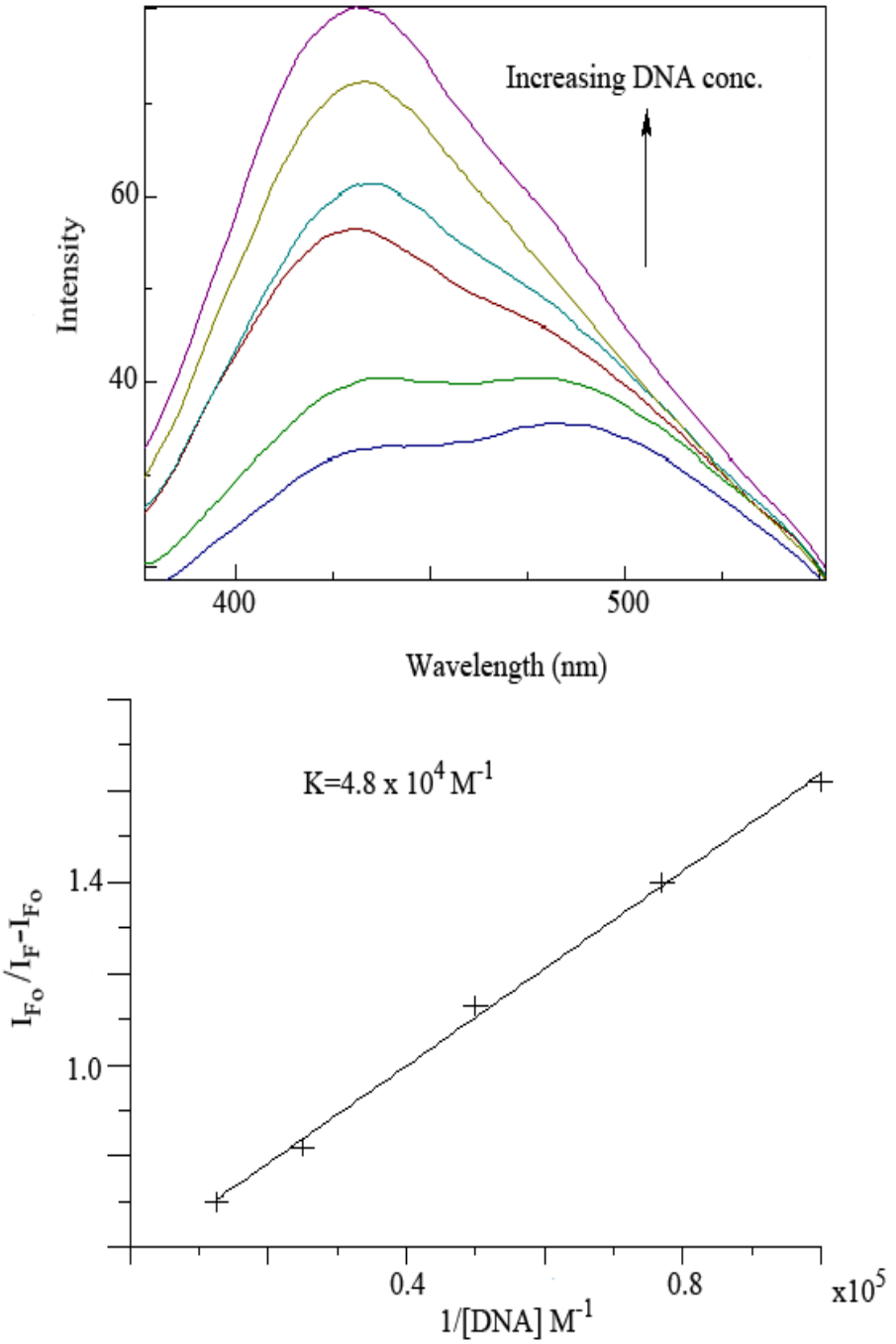

4. Conclusion

Ni(II) complexes with Schiff-bases obtained by the condensation of lysine with salicylaldehyde; 2,3-; 2,4- and 2,5-dihydroxybenzaldehyde and o-hydroxynaphthaldehyde have been synthesized using template method in ethanol or ammonia media. Analytical, magnetic and spectral data show that the Schiff-bases are dibasic tridentate donors and the complexes have square planar and octahedral structures. The complexes thermally decompose in two or three steps where kinetic and thermodynamic parameters of the decomposition steps are computed. The intrinsic binding energy values-calculated using UV and florescence spectroscopy- indicate that the nickel(II) complexes are moderately bind to FM-DNA with almost the same affinity.

References

[1] L.L. Koh, J.O. Ranford, W.T. Robinson, J.O. Svensson, A.L.C. Tan, D. Wu, Inorg. Chem. 35 (1996) 6466-6472.
[2] M.A. Alam, M. Nethaj, M. Ray, Angew. Chem. Int. Ed. Engl. 42 (2003) 1940-1942.
[3] I. Şakíyan, H. Yílmaz, Synth. React. Inorg. Met.-Org. Chem. 33 (2003) 971-983.
[4] B. Sreenivasulu, J.J. Vittal, Inorg. Chim. Acta 362 (2009) 2735-2743.
[5] P.C. Wilkins, R.G. Wilkins, Inorganic Chemistry in Biology, Oxford University Press, Oxford, 1997. 9.
[6] K. Yao, N. Li, Q. Huang, L. Shen, H. Yuan, Sci. China Ser. B42 (1999) 53-61; N. Li, K. Yao, K. Lou, L. Shen, H. Yuan, Sci. China Ser.B 42 (1999) 600-604.
[7] K. Yao, W. Zhou, G. Lu, L. Shen, Sci. China Ser.B 42 (1999) 165-169.
[8] K. Yao, N. Li, L. Shen, Science in China Ser.B 46 (2003) 75-83.
[9] M. Hu, N. Li, K. Yao; Front. Chem. China 4 (2006) 369-373.
[10] Y. Fan, X. He, C. Bi, F. Guo, Y. Yao, R. Chen, Russ. J. Inorg. Chem. 33 (2007) 535-538.
[11] J. Cheng, Q. Lin, R. Hu, W. Zhu, H. Li, D. Wang, Cent. Eur. J. Chem. 7 (2009) 105-110.
[12] M. Begum, S. Saha, M. Nethaji, A. Chakravarty,J. Inorg. Biochem. 104 (2010) 477-484.
[13] B.N. Figgis, J. Lewis: in J. lewis, R.G. Wilkins (eds.), Magnetochemistry of Complex Compounds in Modern Coordination Chemistry, Interscience, New York, 1960).
[14] J. Marmur, J. Mol. Bio. 3 (1961) 208-218.
[15] C.V. Cumar, E.H. Asuncion, J. Am. Chem. Soc. 115 (1993) 8547-8553 .
[16] X. Lu, Q.Y. Lin, X.Q. He, J.Q. Feng, J. Chin. Rare Earth Soc. (2006) 403-407.
[17] R.C. Burrows, J.C. Bailar Jr., J. Am. Chem. Soc. 88 (1966) 4150-4156.
[18] D. Heinert, A. E. Martell, J. Chem. Soc. (1962) 3257.
[19] W. J. Geary, Coord. Chem. Rev. 7 (1971) 81-122.
[20] K. Nakamoto, Infrared and Raman Spectra of Inorganic and Coordination Compounds, Part II: Applications in Coordination, Organometallic, and Bioinorganic Chemistry, 5th ed. Wiley, New York, 1997.
[21] L. Casella, M. Gullotti, J. Am. Chem. Soc. 103 (1981) 6338-6347; I Cavaco, J.C. Pessoa, D. Costa, M.T.L. Durate, R.T. Henriques, P.M.Matias, R.D. Gillard, J. Chem. Soc., Dalton Trans. (1996) 1989-1996; I. Cavaco, J.C. Pessoa, D. Costa, M.T.L. Durate, R.D. Gillard, P.M. Matias, J. Chem. Soc., Dalton Trans. (1994) 149-157.
[22] J. R. Ferrero, Low-Frequency vibrations of inorganic and coordination compounds, Wiley, New York, 1971.
[23] S. Chattopadhyay, M.S. Ray, S. Chaudhuri, G. Mukhopdhyay, G. Bocelli, A.
Cantoni, A. Ghosh, Inorg. Chim. Acta 359 (2006) 1367-1375.
[24] G.A. Melson, D.H. Busch, J. Am. Chem. Soc. 86 (1964) 4830-4833.
[25] W.C.E. Higginson, S.C. Nyburg, J.S. Wood, Inorg. Chem. 3 (1965) 463-467.
[26] L.J. Theriot, G.O. Carlisle, H.J. Hu, J. Inorg. Nucl. Chem. 31 (1969) 2841-2844.
[27] N. Nawar, N. M. Hosny, Trans. Met. Chem. 25 (2000) 1-8.
[28] C. J. Balhausen, An Introduction to Ligand Field, McGrow Hill, New York, 1962.
[29] Y. Özcan, S. Ide, I. Şakíyan, E. Logoglu, J. Mol. Struct. 658 (2003) 207-213.
[30] Z. Rozwadowski, K. Ambroziak, M. Szypa, E. Jagodziňska, S. Spychaj , W. Schilf, B. Kamieňski, J. Mol. Struct. 734 (2005) 137-142.
[31] I. Şakiyan, N. Gűndűz, T. Gűndűz, Synth. React. Inorg. Met.-Org. Chem. 31 (2001) 1175-1187.
[32] O. Carp, D. Gingasu, I. Mindru, L. Patron,

Thermochim. Acta 449 (2006) 55-60.
[33] R. A. Nyquist, R. O. Kagel, Infrared Spectra of Inorganic Compounds, Academic Press, New York and London, 1971.
[34] A.W. Coats, J.P. Redfern, Nature 201 (1964) 68-69.
[35] A. A. Frost, R. G. Pearson, Kinetics and Mechanism - A Study of Homogenous Chemical Reaction, Wiley, New York, 1961.
[47] H. A. Benesi, J. H. Hildebrand, J. Am. Chem. Soc. 71 **(**1949) 2703-2707.
[48] C. Yu, Y. Shao, N. Gan, Q. Xu, Z. Guo, Inorg. Chem. 43 (2004) 4761-4766.
[49] M. Baldini, M. Belicchi-Ferrari, F. Bisceglie, G. Pelosi, S. Pinelli, P. Tarasconi, Inorg. Chem. 42 (2003) 2049-2055.
[50] M. Cory, D.D. Mckee, J. Kagan, D.W. Henry, J.A. Miller, J. Am. Chem. Soc. 107 (1985) 2528-2536.
[51] S. Satyanarayana, J.C. Dabrowiak, J. B. Chaires, Biochemistry 31 (1992) 9319-3924.
[52] F. Arjmand, B. Mohani, S. Ahmad, Eur. J. Med. Chem. 40 (2005) 1103-1110.
[53] J.M. Kelly, A.B. Tossi, D.J. McConnel, T. C. Strekas, Nucleic Acid Res. 13 (1985) 6017-6034.